HIGH FREQUENCY LUMPED PARAMETER MODEL FOR AC MOTOR WINDINGS

G. Grandi *, D. Casadei *, A. Massarini **

* Dept. of Electrical Engineering, viale Risorgimento 2 , 40136, Bologna - Italy
** Dept. of Engineering Sciences, via Campi, 203/B, 41100, Modena - Italy

Abstract. The paper describes a HF equivalent circuit for the stator winding of three-phase AC motors, valid in a wide frequency range. The model fitting is based on winding complex impedance measurements. Both the phase-to-phase and the phase-to-ground impedances are considered. The proposed model can be utilized in theoretical and numerical HF analysis of inverter-fed AC motors. In this case, the equivalent circuit allows to predict both differential- and common-mode conducted EMI. Furthermore, also transient effects can be predicted when the analysis is performed in the time domain. The numerical results, obtained by means of PSpice, are compared with the corresponding experimental tests in both frequency and time domains.

Keywords. HF model, equivalent circuit, AC winding, conducted EMI

INTRODUCTION

In recent years, inverter motor drives have become the most popular systems to handle electromechanical power conversion. The modern power converters are based on switching mode operation with static components of the last generation. The static switches, such as MOSFETs and IGBTs, are characterized by very fast commutations (i.e., fractions of μs). The switching frequency is usually fixed in the range of tens of KHz to avoid acoustic noise. As a consequence, undesired harmonic voltage components can range from tens of KHz to several MHz. These High Frequency (HF) voltage harmonics are responsible of HF currents. The propagation path of the current harmonics is rather unexpected owing to stray and parasitic motor parameters that take importance at high frequency. Thus, a circuit model of the motor windings is particularly useful to predict HF current components and, in general, conducted Electro-Magnetic Interferences (EMI) [1]. Since the motor frame is usually grounded, both differential- and common-mode EMI must be considered.
In the low and medium power range, the low voltage induction motor is the most frequently used type of motor. The windings of this type of motor are usually realized by a series connection of mush wound coils. A winding model consisting in a cascade connection of single-coil models can be particularly useful to determine the fast fronted voltage distribution among the coils [2]-[6]. Owing to the random distribution of the turns in each coil, an analytical evaluation of the coil model cannot be based on single-turn models such as in form wound coils. Hence, the lumped equivalent circuit of a coil can be defined in terms of equivalent impedance by a proper three-terminal circuit. Both the real and imaginary components of the impedance [7] or only the impedance magnitude [8] can be considered. In this paper the main results obtained in [7] are summarized and extended to the case of multi-coil stator windings with reference to three-phase induction motors.

SINGLE COIL MODEL

A detailed analysis of single-coil stator windings has been presented in [7] leading to the lumped parameter model represented in Fig. 1.

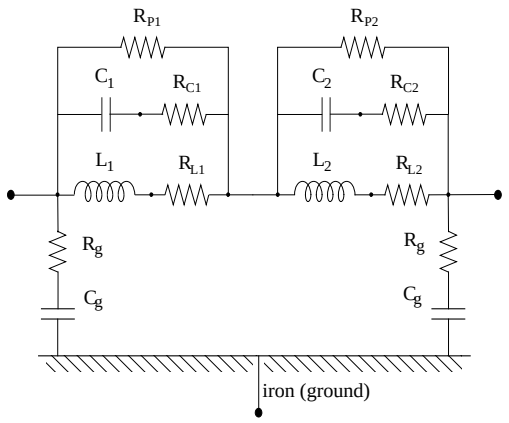

Fig. 1: HF equivalent circuit of a mush wound coil

The coil is regarded as a series connection of N turns having a circular cross section. The distribution of the N turns is random in both the slot region and the overhang region. The coil geometry and the coil cross section in the slot region are given in Fig. A1 of the Appendix.

Background

The HF circuit model of a mush wound coil proposed in [7] considers both turn-to-turn and turn-to-iron capacitances. Also additional dissipative phenomena such as skin and proximity effects in the wires, dielectric and iron losses are taken into account. The proposed approach is based on the equivalence between the coil and the circuit model in terms of complex impedance $\mathbf{Z}_C$. Hence, both the real part (equivalent series resistance) and the imaginary part (equivalent series reactance) of $\mathbf{Z}_C$ are considered.
Experimental tests on several coils have been carried out, showing in all cases a pair of more or less smoothed

parallel resonances in the considered frequency range. Furthermore, very large dissipative phenomena associated with the resonances have been observed. The equivalent circuit shown in Fig. 1 allows the frequency response of the coil to be represented in a satisfactory manner when the circuit parameters are properly evaluated.

Model parameter evaluation

To make the model fit with the experimental results an identification problem has to be solved. The identification procedure can be carried out by a simple trial and error method or more sophisticated numerical techniques such as the least squares method. The complex admittances between the two coil terminals ($\mathbf{Y}_c$) and between a coil terminal and the stator frame ($\mathbf{Y}_g$) can be expressed as a function of the model parameters and the excitation angular frequency (ω) as follows

$$\mathbf{Y}_c = \frac{1}{\mathbf{Z}_c} = \frac{1}{2R_g + \dfrac{2}{\mathbf{j}\omega C_g}} + \frac{1}{\mathbf{Z}_1 + \mathbf{Z}_2} \qquad (1)$$

$$\mathbf{Y}_g = \frac{1}{\mathbf{Z}_g} = \frac{1}{R_g + \dfrac{1}{\mathbf{j}\omega C_g}} + \frac{1}{\mathbf{Z}_1 + \mathbf{Z}_2 + \left(R_g + \dfrac{1}{\mathbf{j}\omega C_g}\right)},$$

where $\mathbf{Y}_1$ and $\mathbf{Y}_2$ are given by

$$\mathbf{Y}_1 = \frac{1}{\mathbf{Z}_1} = \frac{1}{R_{p1}} + \frac{1}{R_{L1} + \mathbf{j}\omega L_1} + \frac{1}{R_{C1} + \dfrac{1}{\mathbf{j}\omega C_1}} \qquad (2)$$

$$\mathbf{Y}_2 = \frac{1}{\mathbf{Z}_2} = \frac{1}{R_{p2}} + \frac{1}{R_{L2} + \mathbf{j}\omega L_2} + \frac{1}{R_{C2} + \dfrac{1}{\mathbf{j}\omega C_2}}.$$

An initial estimate of the main circuit parameters can be performed using the procedure presented in [7]. A brief description of this procedure is given below.

Overall coil inductance. As it is shown in Fig. A1, the coil consists of two semi-circular or rectangular parts in the overhang region, connected by two parallel straight parts in the slot region. We assume the coil inductance L as the sum of the inductance L^{air} of the wires in the overhang region and the inductance L^{iron} of the wires in the slot region. This assumption is satisfied with a good approximation. In fact, the flux lines produced by the overhang conductors mainly lie in planes perpendicular to the iron lamination. These flux lines do not penetrate the iron core owing to the shielding effect of the eddy currents which can freely circulate in the iron sheets.
On the basis of the previous considerations, we can calculate the inductance L^{air} by the image method related to a current in presence of a planar magnetic shield [9]. In the case of semi-circular overhangs, the inductance can be calculated as the inductance of a single circular loop of diameter D_h

$$L^{air} = \frac{\mu_o D_h}{2}\left(\ln\frac{8D_h}{D_c} - \frac{7}{4}\right)N^2. \qquad (3)$$

In the case of rectangular overhangs, the method of partial inductance can be adopted [10] to calculate the inductance L^{air}.
With reference to the inductance L^{iron}, we can note that this contribution is strongly affected by the frequency. In this case the lamination opposes the eddy currents so that the shielding effect becomes significant only at high frequencies. It has been verified that only for frequencies above several MHz the magnetic field is completely rejected outside the laminated iron core. For this reason, the determination of the coil inductance requires an accurate and complex field analysis taking eddy current and iron lamination into account. However, neglecting the magnetic field penetration inside the laminated iron-core, the inductance L^{iron} can be evaluated as the inductance of a group of N parallel straight conductors having length $2d_{ir}$, and surrounded by a cylindrical shield. This assumption leads to

$$L^{iron} = \frac{\mu_o}{\pi}\left(\frac{1}{4} + \ln\frac{D_s}{D_c}\right)d_{ir}\,N^2. \qquad (4)$$

The inductance measurements can be performed only up to few tens of kHz due the parallel resonances caused by turn-to-turn and turn-to-iron parasitic capacitances. A method to extend the inductance measurements to the high frequency range is described in [7]. It consists of inductance measurements on coils with a reduced number of turns. In this way the parasitic capacitive effects are reduced and the parallel resonances are shifted at higher frequencies. Then, the coil inductance can be calculated by an extrapolation procedure. It has been verified that the sum of the values calculated by (3) and (4) represents the asymptotic lower limit of the extrapolated values.

Coil capacitances. An analytical evaluation of the coil capacitances, such as in [11], is prevented by the random distribution of the turns in mush wound coils.
The overall coil-to-ground capacitance C_{tg} can be evaluated by short-circuiting the coil terminals and measuring the capacitance between the resulting node and the motor frame. In the equivalent circuit of Fig. 1, the capacitive coupling to ground is represented by the two capacitances $C_g = C_{tg}/2$ connected at the beginning and the end of the coil.

Coil losses. The coil losses are taken into account by series and parallel resistances. The sum of R_{L1} and R_{L2} represents the AC wire resistance. The values of these resistances are function of the excitation frequency owing to skin and proximity effects. However, in order to obtain an equivalent circuit which can be readily utilized for both frequency and time domain analyses, these resistances are fixed at average values (hundreds of Ohm). R_{p1} and R_{p2} take account of the AC iron losses and the corresponding values are in the order of KΩ or tens of KΩ. R_{C1}, R_{C2}, and R_g are introduced to model the dissipative phenomena due to HF capacitive currents, and dielectric losses. Usually their values are in the order of tens of Ohm.

DETAILED WINDING MODEL

For the considered AC motor size (i.e., from fractions of kW up to few tens of kW), the stator windings are built as a series connection of mush wound coils. In order to obtain the circuit model of the motor windings, a cascade connection of coil models can be considered. In order to evaluate the inductive and capacitive couplings among the coils, either numerical or experimental approaches can be employed.

Inductive couplings

The numerical evaluation of the mutual inductances among the coils is a hard task due to the presence of a laminated iron core. In fact HF eddy currents can flow in the iron core despite of the iron lamination. As a consequence, the mutual inductances change as a function of the excitation frequency. The calculation of the mutual inductances can be performed by neglecting the magnetic penetration depth in the iron core and considering the coupling in the overhang region only. This value corresponds to the asymptotic lower limit of the mutual inductance obtained for frequencies above 1 MHz. With reference to rectangular overhangs, an extension of the method of "partial inductance" [10] can be usefully employed to evaluate the mutual couplings.
As in the case of single-coil analysis, the parallel resonances limit the maximum frequency at which the mutual inductance measurements can be performed.
Although there are impedance bridges that can measure the mutual inductance, a common method to determine M is based on measuring the equivalent inductance with different coil connections. This procedure leads to

$$M = \frac{L' - L''}{4} \tag{5}$$

where L' and L'' represent the measured inductances when the two coils are connected in series with positive and negative mutual coupling, respectively.

Capacitive couplings

The random distribution of the coil turns prevents either analytical or numerical calculations of coil-to-coil and coil-to-ground capacitances. A detailed measurement of these capacitances requires particular technique to be adopted owing to the complexity of the parasitic capacitance network. In order to decouple the coil-to-coil and coil-to-ground capacitances, the coils terminals must be properly connected. As an example, in order to evaluate the coil-to-ground capacitance, it is convenient to connect all the coil terminals at the same node and measure the overall capacitance between the node and the ground. In this way both the coil-to-coil and the inner coil capacitances are short-circuited. Thus, the coil-to-ground capacitance of a single coil can be readily obtained dividing the measured capacitance by the total number of coils.
The equivalent circuit of the motor windings based on series connections and couplings among single-coil models results in a very complex electrical network. Furthermore, the high number of the circuit parameters makes burdensome the model fitting. On the other hand, this detailed model can be usefully employed when the transient voltage distribution among the coils has to be predicted or analyzed. In particular, the coil voltage drop can be considered as the worst case in terms of maximum voltage between adjacent turns. In this way, the maximum electrical stress in the winding interturn insulation can be predicted. This is the case when the enameled wires at the beginning and at the end of a coil touch one another [12]. The effects of fast-fronted electrical fields in the stator winding insulation have been discussed in terms of existence of partial discharges in [12] and [13].

SIMPLIFIED THREE-PHASE WINDING MODEL

When the analysis of the voltage distribution among the coils is not required, a simplified equivalent circuit for the motor winding can be defined. In this case the AC motor can be regarded as a "black box" with one terminal for each motor phase and a terminal for the motor frame (ground). Thus, the equivalence is formulated in terms of phase-to-phase and phase-to-ground complex impedances. Some impedance measurements on different stator windings have shown that the same topology of the single-coil equivalent circuit (Fig. 1) can be adopted also for each phase of the AC motor. In this case, the mutual coupling among the phases should be introduced. In this paper the inductive couplings among the phases are taken into account by mutual coefficients (M_1 and M_2). The direct phase-to-phase capacitive couplings have been neglected being the corresponding capacitances much lower then the phase-to-ground capacitances. The resulting model valid for three-phase motor windings is represented in Fig. 2.

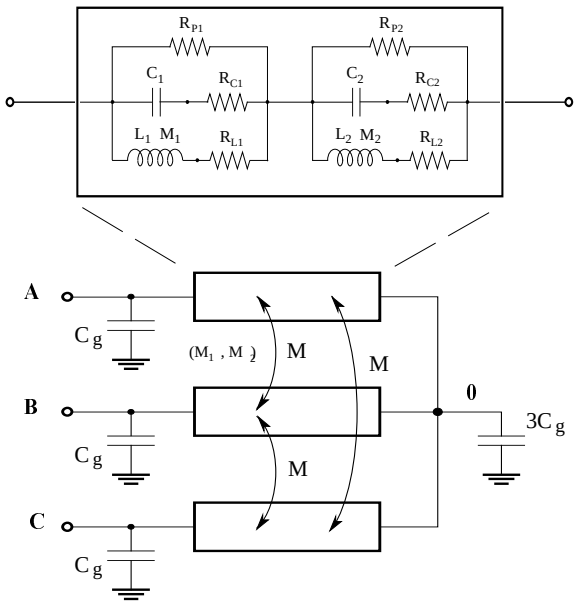

Fig. 2: Scheme of the three-phase winding model

In order to make the three-phase winding model fit with the experimental data, an identification problem has to be solved. The problem is equivalent to that of the single-coil model discussed at the beginning of this paper and in [7].

Frequency Response

Phase-to-phase

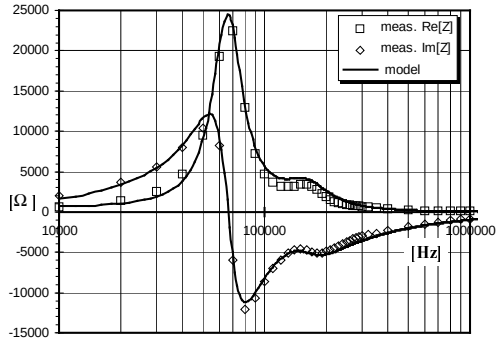

Fig. 3: Real and Imaginary impedance components

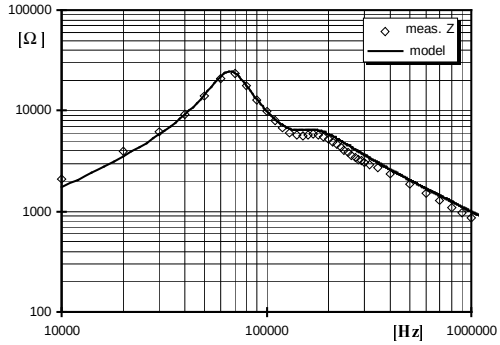

Fig. 4: Impedance magnitude

Phase-to-ground

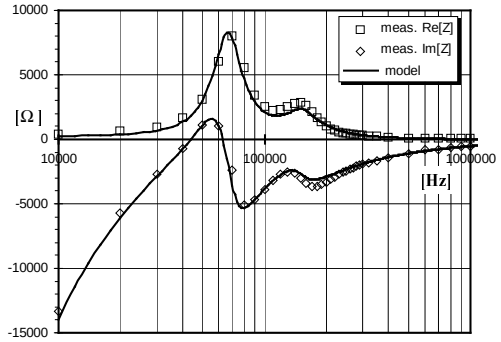

Fig. 5: Real and Imaginary impedance components

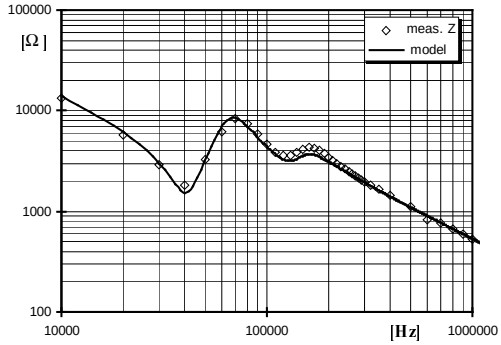

Fig. 6: Impedance magnitude

An initial estimate of the reactive parameters of the three-phase model can be obtained by the following procedure.

Self- and mutual phase inductances. The overall phase inductance $L_p = L_2+L_2$ can be evaluated by impedance measurements at the phase terminals for frequencies lower than the first resonant frequency. This parameter is frequency-dependent but an average value can be extrapolated and fixed in the considered frequency range. The mutual inductance M between two motor phases can be evaluated by (5) using the procedure described above.

Phase-to-ground capacitances. The capacitive coupling between each motor phase and the ground is represented by two lumped capacitances C_g at the beginning and the end of each phase (Fig. 2). These capacitances can be evaluated by connecting the six terminals of the phases at the same node and measuring the overall node-to-ground capacitance C_{tg}: $C_g = C_{tg}/6$. C_{tg} corresponds to the capacitance between one phase terminal and the ground measured at a low frequency (e.g., below the resonances). In fact, for either delta or star connections, the phase inductive reactances are negligible with respect to the capacitive parallel reactances.

Inner phase capacitances. With reference to Fig. 2, the input-to-output inner phase capacitance C_p is represented, for high excitation frequencies (e.g., above the resonances), by the series of the capacitances C_1 and C_2 of the two resonators. The evaluation of this capacitance can be carried out by measuring the capacitance C_{tp} between two phase terminals at a high frequency. Assuming star connected motor phases yields

$$C_{tp} = \frac{1}{2}\left(C_g + C_p\right) \quad \Rightarrow \quad C_p = 2\,C_{tp} - C_g\,.$$

Both L_p and C_p must be splitted into L_1, L_2, and C_1, C_2, respectively, according to the equivalent circuit of Fig. 2. As a first order approximation, this can be done by imposing the frequency of the two parallel resonances.

EXPERIMENTAL TESTS

In order to verify the proposed model for three-phase motor windings, frequency and time domain measurements have been performed on a test motor. The rated characteristics of the motor are given in Table 1 of the Appendix. The behavior of both phase-to-phase and phase-to-ground impedances has been investigated.

Frequency domain analysis

The measurements have been performed by a programmable RLC meter HP 4192 with the frequency ranging from 10 KHz to 1 MHz. The parameter values obtained by the fitting procedure are given in Table 2 of the Appendix. The corresponding calculated and measured impedances are represented from Fig. 3 to Fig. 6. The solid lines represent the numerical results whereas the markers indicate the measured values. Figs. 3 and 4 are related to phase-to-phase impedance (A-B). Figs. 5 and 6 illustrates the results of phase-to-ground impedance (A-g). It can be noted that the agreement between numerical and experimental data is good in a wide frequency range despite of the model fitting which has been performed by a simple trial and error procedure. In this case, the model accuracy could be further improved by numerical techniques.

Transient Analysis

(a) - Numerical results **(b) - Experimental results**

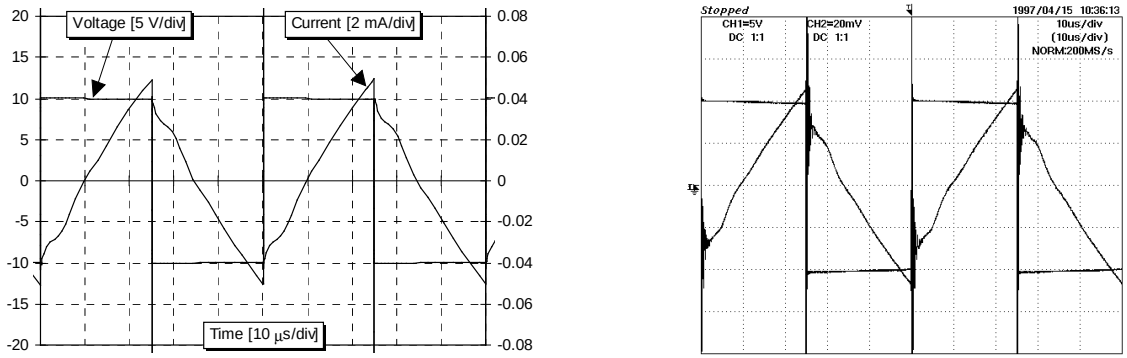

(a) Fig. 7: Phase-to-phase rectangular voltage (b)

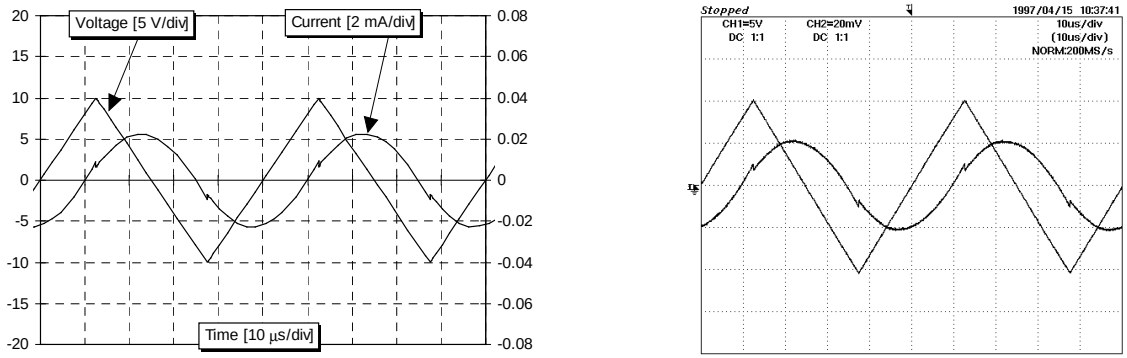

(a) Fig. 8: Phase-to-phase triangular voltage (b)

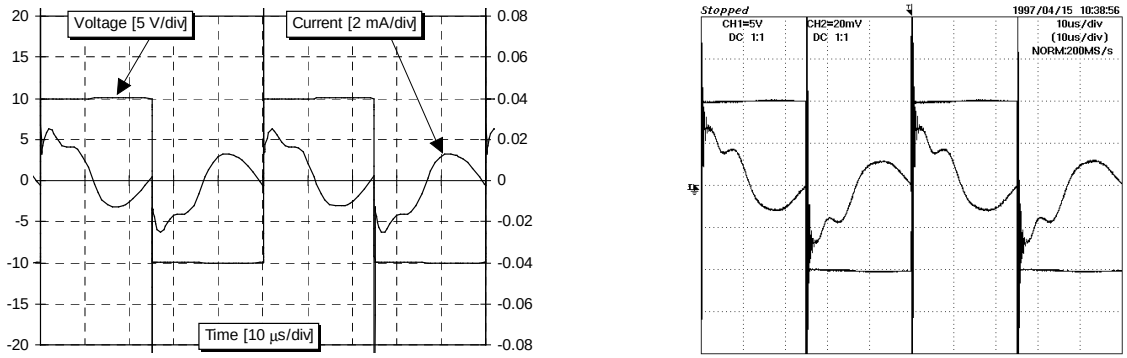

(a) Fig. 9: Phase-to-ground rectangular voltage (b)

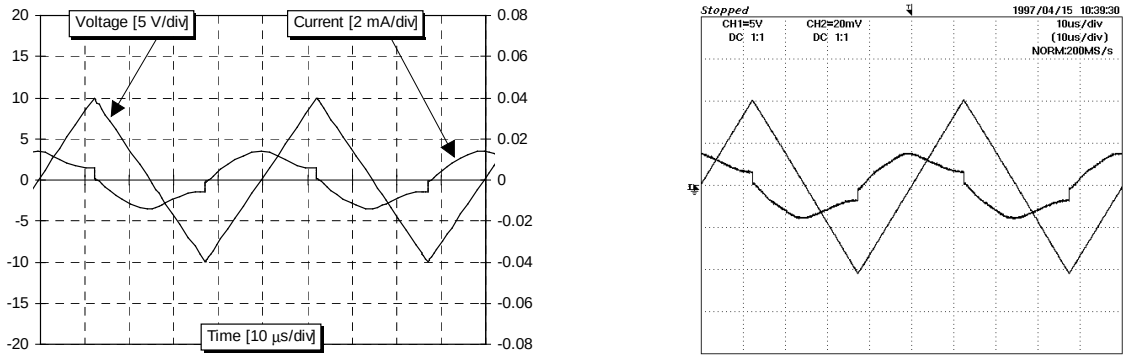

(a) Fig. 10: Phase-to-ground triangular voltage (b)

Time domain analysis

The transient analysis has been performed by supplying the motor with a proper voltage source and measuring the resulting phase current. As test signals, both rectangular and triangular voltage waveforms have been adopted (20 kHz). The current signal is represented by the voltage across a 10 Ω shunt resistance.
The corresponding numerical and experimental results are shown from Fig. 7 to Fig. 10. The agreement is good even if the dependence of all the model parameters on the excitation frequency has been neglected. This assumption allows numerical simulations to be achieved by PSpice with a very low computational time (few seconds).

CONCLUSIONS

The proposed HF lumped equivalent circuit for AC motor stator windings is valid in a wide frequency range. The model fitting is based on phase-to-phase and phase-to-ground (frame) impedance measurements. The real and imaginary impedance components have been separately considered. A method to achieve an initial estimate of the reactive model parameters has been proposed. A simple trial and error procedure has been employed for the parameter identification leading to a good agreement between calculated and experimental results. More sophisticated numerical methods could be also employed to improve the model accuracy.
By the equivalent circuit presented in this paper both frequency and time domain analyses can be performed. The model is particularly useful to determine differential- and common-mode conducted EMI in the case of inverter-fed AC motors.

REFERENCES

[1] E. Zhong, S. Chen, T.A. Lipo, "Improvements in EMI Performance of Inverter-Fed Motor Drives," *Proc. of APEC*, March 1994, pp. 608-614.

[2] M.T. Wright, S.J. Yang, K. McLeay, "General Theory of Fast-Fronted Interturn Voltage Distribution in Electrical Machine Windings," *IEE Proc. Part. B*, Vol. 130, No. 4, July 1983, pp. 245-256.

[3] J.L. Guardado, K.J. Cornick, "A Computer Model for Calculating Steep-Fronted Surge Distribution in Machine Windings," *IEEE Trans.*, Vol. EC-4, No.1, March 1989, pp. 95-101.

[4] H. Oraee, P.G. McLaren, "Surge Voltage Distribution in Line-End Coils of induction Motors," *IEEE Trans.*, Vol. PAS-104, No. 7, July 1985, pp. 1843-1848.

[5] R.G. Rhudy, E.L. Owen, D.K. Sharma, "Voltage Distribution Among the Coils and Turns of a Form Wound AC Rotating Machine Exposed to Impulse Voltage," *IEEE Trans*., Vol. EC-1, No. 2, June 1986, pp. 50-60.

[6] L. Gubbala, A. von Jouanne, P. Enjeti, C. Singh, H. Toliyat, "Voltage Distribution in the Windings of an AC Motor Subjected to High dv/dt PWM Voltages," *Proc. of PESC Conference*, June 1995, Atlanta, pp. 579-585.

[7] G. Grandi, D. Casadei, U. Reggiani, "Equivalent Circuit of Mush Wound AC Windings for High Frequency Analysis," *Proc. ISIE Conf.*, July 1997, Guimarães (Pt)

[8] A. Consoli, G. Oriti, A. Testa, A.L. Julian, "Induction Motor Modeling for Common Mode and Differential Mode Emission Evaluation," *Proc. of IAS Conference*, October 1996, Vol. 1, pp. 595-599.

[9] H.A. Haus and J.R. Melcher: *Electromagnetic Fields and Energy*. Prentice Hall, New Jersey: 1989.

[10] C.R. Paul: *Electromagnetic Compatibility*. John Wiley, New York: 1992.

[11] G. Grandi, A. Massarini, M.K. Kazimierczuk, U. Reggiani, "Capacitances of Single-Layer Air-Core Inductors for High-Frequency Applications," *Proc. of IAS Conference*, October 1996, Vol. 3, pp. 1384-1388.

[12] M. Kaufhold, G. Borner, M. Eberhardt, J. Speck, "Failure Mechanism of the Interturn Insulation of Low Voltage Electric Machines Fed by Pulse-Controlled Inverters," *IEEE - E.I. Magazine*, Sept/Oct 1996, pp. 9-16.

[13] A. Mbaye, F. Grigorescu, T. Lebey, Bui Ai, "Existence of Partial Discharges in Low-voltage Induction Machines supplied by PWM Drives," *IEEE Trans. on DEI*, Vol. 3, No.4, August 1996, pp. 554-560.

APPENDIX

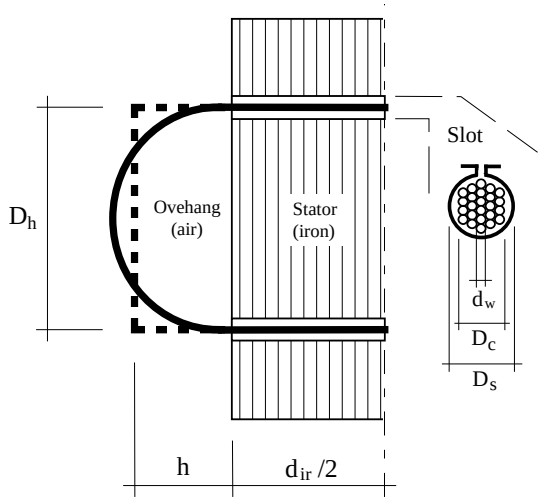

Figure A1: Coil geometry and details of a slot cross section.

TABLE 1 - Three-phase induction motor data

rated power	1.5 kW
rated voltage	380 V (Y)
rated frequency	50 Hz

TABLE 2 - Three-phase model parameters

R_{L1} = 150 Ω	R_{p1} = 11 kΩ	C_1 = 380 pF	L_1 = 7.3 mH
R_{L2} = 150 Ω	R_{p2} = 5 kΩ	C_2 = 220 pF	L_2 = 3 mH
R_{C1} = 15 Ω	R_g = 10 Ω	C_g = 183 pF	M_1 = -2.6 mH
R_{C2} = 10 Ω			M_2 = 0 mH